Effect of the Number Shots of Laser on Structural Transformations and Optical Properties of ZnS Nanoparticles Thin Films

A.Z. Mohammed[1], N.J. Mohammed[2*], I.K. Khudhair[2]
[1] Physics Department, Faculty of Science, Zagazig University, Zagazig, Egypt
[2] Physics Department, Faculty of Science, Al-Mustansiriyah University, Iraq

Effects of the number of shots of laser and annealing temperature on the structural, morphological, and optical properties of zinc sulfide nanoparticles (ZnS NPs) thin films, prepared by pulsed laser deposition technique (PLD), were investigated. XRD results show that ZnS NPs exhibit a hexagonal phase at 623k. Transformation in the shape of nanoparticles to nanoflowers and nanorods appeared with increasing number of shots of laser at the same annealing temperature (623K) was observed from scanning electron microscopy (SEM) images. The optical properties were studied from all transmittance data. The experimental results show that the as-deposited ZnS NPs film exhibit a cubic structure and the crystallinity increased in the annealed films. It is also found that the grain size of the as grown samples at 300K, rises linearly from 9 to 11 nm with increasing the number of shots from 1000 to 3000 and rapidly from 10 to 18 nm after annealing at 623K. Additionally, the increase of the number of shots from 1000 to 3000 leads to a decrease in the energy gap values and increases their values after heat treatment keeping their behavior decreasing as the number of shots of laser increases. Also, photoluminescence (PL) measurements explained quenching its value after annealing temperature.

Keywords: ZnS, Pulsed laser deposition, Nanoparticles, Nano leaves, Nanoflowers, Nanorods, Photoluminescence (PL), Annealing temperature

Introduction

ZnS is a II-VI compound semiconductor. It is widely applied in the optoelectronic applications consisting of light emitting diodes with short wavelength. The structure and properties of ZnS films vary according to the deposition technique. Many growth techniques have been reported to prepare ZnS thin films, such as sputtering [1], Pulsed-laser deposition [2], metal organic chemical vapor deposition [3], electron beam evaporation [4], photochemical deposition [5], and chemical bath deposition [6]. Among these methods, electron beam evaporation is the most interesting. The advantages of electron beam evaporation are stability, reproducibility; high deposition rate, moreover, the compositions of the films are controllable. ZnS is one of the first semiconductors discovered [7], and is also an important

semiconductor material with direct wide band gaps for cubic and hexagonal phases of 3.72 and 3.77 eV, respectively [8]. ZnS has a high absorption coefficient in the visible range of the optical spectrum and reasonably good electrical properties [9]. In recent years, ZnS thin films have been grown by a variety of deposition techniques, such as chemical bath deposition [10], evaporation [11], and solvo thermal method [12]. Chemical bath deposition is a promising technique because of its low cost arbitrary substrate shapes, simplicity, and capability of large area preparation. There are many reports of successful fabrication of ZnS-based hetero-junction solar cells by utilizing the chemical bath deposition method, such as with CIGS used for the n-type emitter layer [13]. The much pulsed laser deposition experiments were carried out in the 1960s, however it was first

popularized during the 1980s by the work of Inamet et al. [14], who deposited high temperature super conducting films with a complex stochiome ZnS is potentially important material to be used as an antireflection coating for hetero-junction solar cells [15]. In this research A novel method was used involving changing the number of shots of laser to produce ZnS NPs, nanoflowers and nanorods at the same heat treatment temperature (623K) without inlet gas to the vacuum chamber.

Experimental

The ceramic ZnS target used is a pellet with dimensions (2 cm x 0.1 cm), density 3.66 g /cm^3 and purity 99.99%, supplied by the Kurt J. Lesker Company. It is produced by pressing squeeze at 13 ton, and sintering ZnS powder under vacuum at 1125K. It is a suitable target for PLD since it is dense and flat, enabling uniform energy transfer to its surface and the absence of voids keeps large particles being ejected from the surface. ZnS NPs films were prepared by pulsed laser deposition system of ZnS pellet fixed to a target holder that located at 2 cm and parallel to the substrate surface. The PLD was carried out by using a Q-

switched Nd: YAG laser with wave length (1064 nm), number of shots of laser (1000, 2000, 3000), laser flounce (16.98 J/cm^2) and spot (d=3mm) at an angle 0f 45°. The repetition rate of the laser beam was 5 Hz. The target and substrate were rotated at 10 and 6 rpm respectively, by using DC motor to avoid drilling effect. The chamber of substrate and target holder evacuated to a pressure about 10^{-5} mbar. The preparation temperatures of samples were as grown temperature (300K) and annealing temperature (623K). In a typical case (16.98 J/cm^2, 1064 nm) the thickness created after deposition by 1500 pulses was found to be 50 nm.

Results & Discussion

The structure of ZnS target was investigated using X-ray diffraction, as shown in Figure (1), and it was found that ZnS exhibits hexagonal phase. ZnS NPs thin films were prepared in an evacuated chamber to a base pressure of (10^{-5} mbar). All three films, prepared by different number of shots of laser (1000, 2000, and 3000) at room temperature (300K), were annealed at 623K. The crystal structure of the films was examined by X-ray diffraction (XRD) as shown in Figure (2).
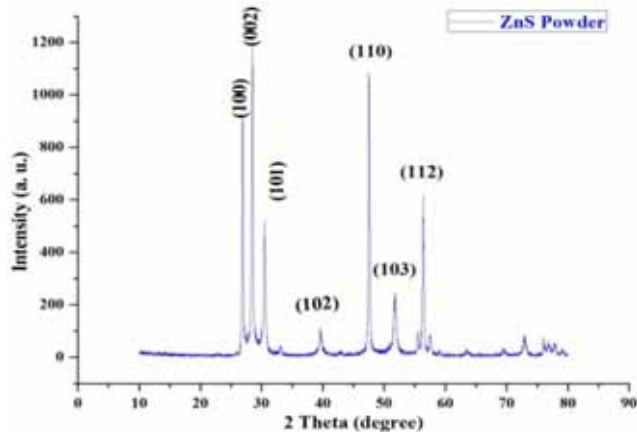

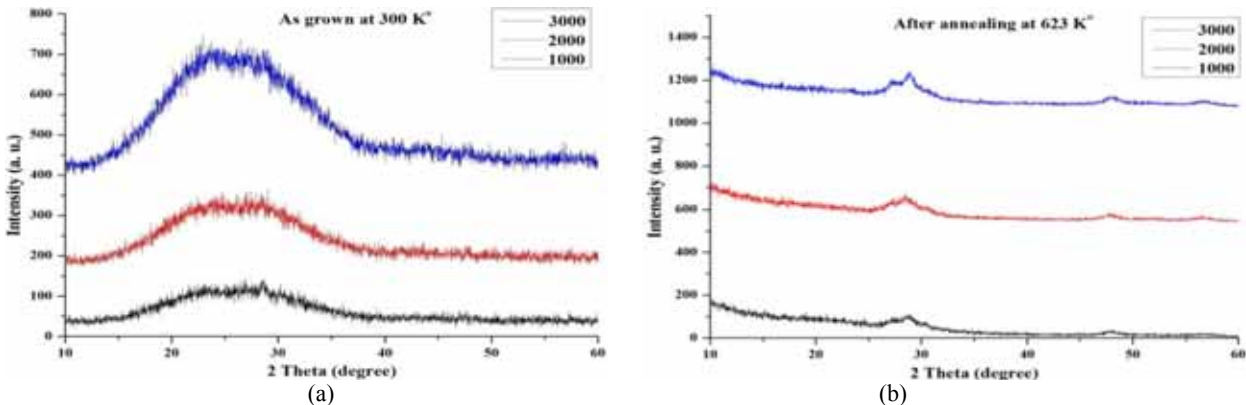**Figure (1): X-ray diffraction patterns for ZnSta target**

(a)   (b)

Figure (2): X-ray diffraction patterns for ZnS NPs films at a) as grown 300K, b) annealed at 623K

The average crystallite size (D) of ZnS NPs was estimated by the standard Scherrer formula [16]
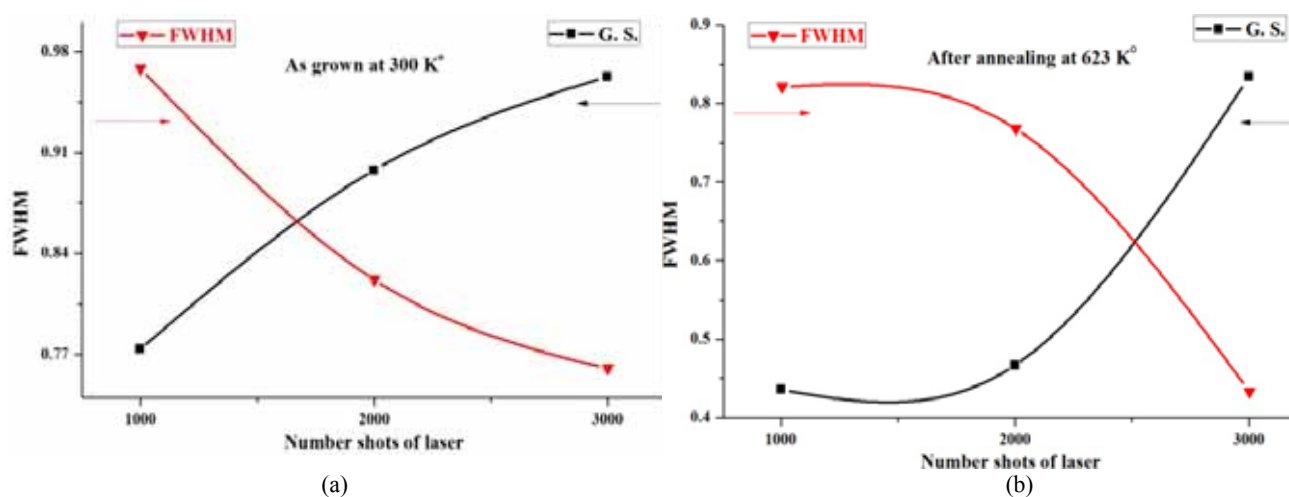
$$D = \frac{k\lambda}{\beta cos\theta} \qquad (1)$$

Where k is constant$(0.89 < k > 1)$, β is the Full Width at Half Maximum (FWHM) of the diffraction peak, λ is the wavelength of the X-ray and θ is diffraction angle. At different no. shots of laser (1000, 2000, 3000), it can be observed that the crystallite size of the samples increased after annealing from (9, 9.5, 11nm) at (300K) to (10, 11, 18 nm) at 623K.as shown in Figure (3).

Also, it can be noticed that the differences in the crystallite size at 300K and at annealed temperature (623K) increased with increasing no. of pulses as shown in Fig (4).

Further investigations on the characteristics of nanosized structures of the deposited materials were achieved using atomic force microscopy. The AFM image of the ZnS NPs thin films deposited by different no. shots (1000, 2000, 3000) at 300K are shown in Figure(5).

The AFM image of the ZnS NPs thin films deposited by different number of shots (1000, 2000, and 3000) after annealed at 623K is illustrated in Figure(6).

(a)

(b)

Figure(3): The crystallite size verse FWHM of ZnS NPs films for different no. shots (1000, 2000, 3000) at: a) as grown 300K, b) annealed at 623K
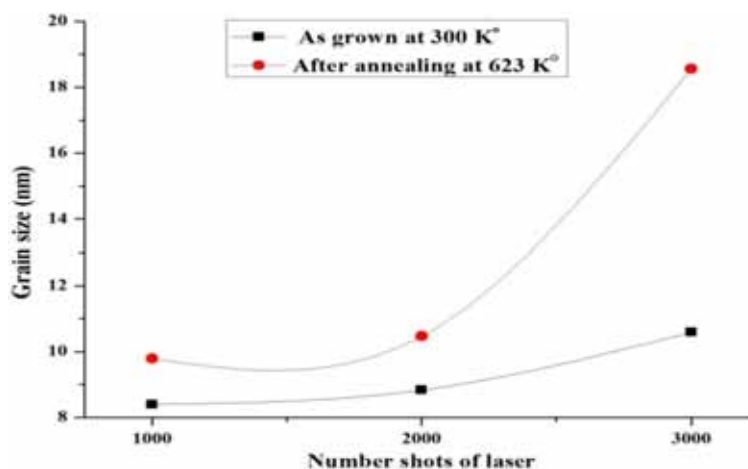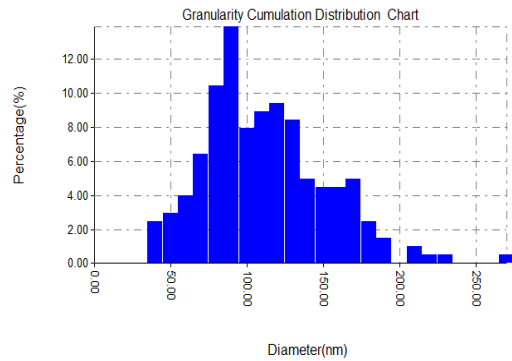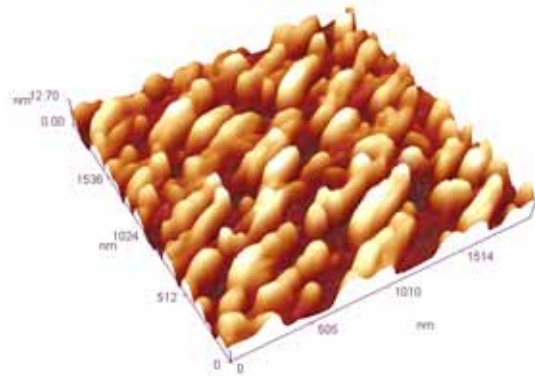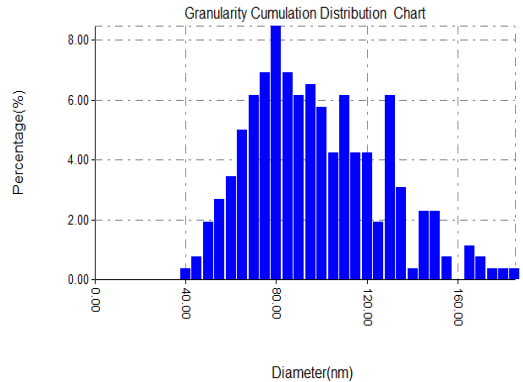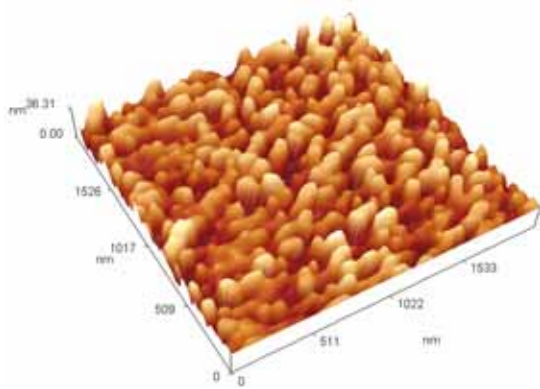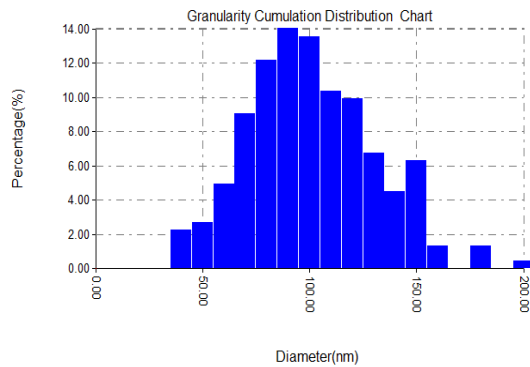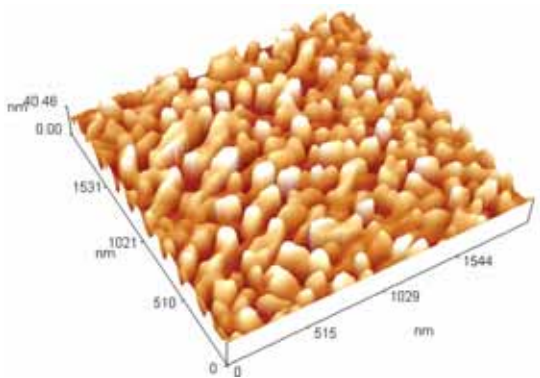

Figure (4): The differences in the crystallite size at 300K and at annealing temperature (623k)

Avg. Diameter : 107.96 nm

Avg. Diameter: 94.93nm

Avg Diameter 95.95nm

Figure (5): AFM of ZnS NPs thin films deposited by different shots (1000, 2000, 3000) with average grain size (107.96, 94.93 and 95.95nm) respectively at 300k before annealing

Avg. Diameter:89.01nm
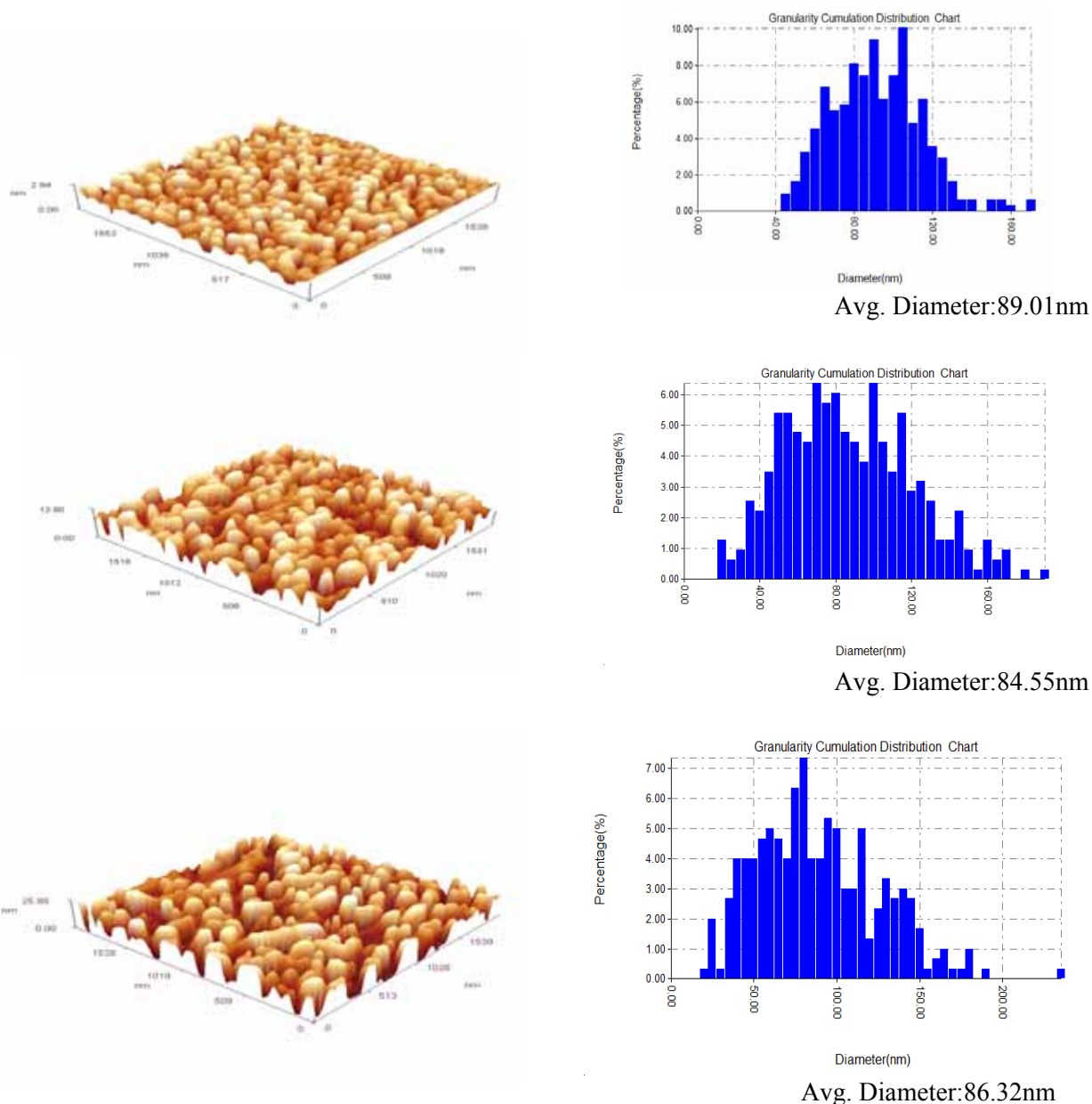

Avg. Diameter:84.55nm

Avg. Diameter:86.32nm

Figure (6): AFM of ZnS NPs thin films deposited by different shots (1000, 2000, 3000) with average grain size (89.01, 84.55 and 86.32 nm) respectively after annealing at 623K
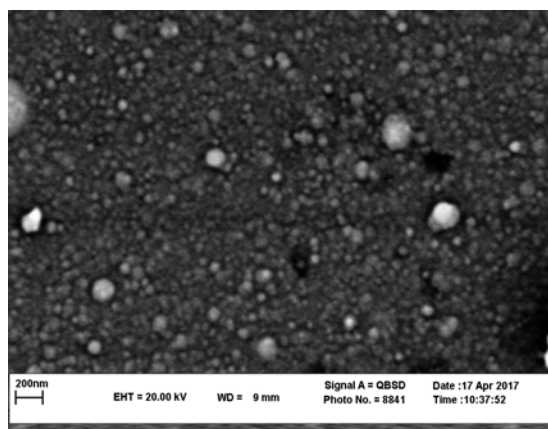
The average size of ZnS NPs was about 99 nm at 300K and the average size decreased to 86 nm after annealing samples at 623K. The root mean square (rms) surface roughness at 300K for the prepared films with different no. shots (1000, 2000, and 3000) are 3.61, 7.78 and 8.36 nm respectively. After annealing the samples at 623K the (rms) the surface roughness decreased for each sample and increased with increasing number of shots of laser for all samples. Table (1) shows the surface roughness of ZnS NPs thin film deposited on glass substrate. Increasing number of shots

leads to an increased roughness of the surface and increasing the temperature could reduce it. The decrease in (rms) surface roughness may be due to the decrease in the number of point defects which means a decrease of dislocations density (δ) in the films as shown in Table (1).
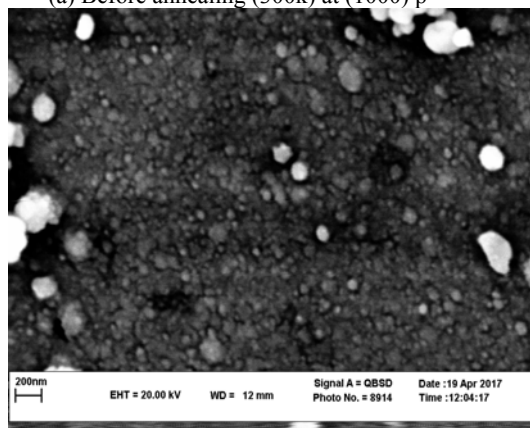
The SEM images are presented in Figure(7) as a function of the number of shots of laser and annealing temperature. Figure7(a) shows the SEM image of a synthesized sample at 300K for 1000 shots, the nanoparticles transformed from circular to nanoflowers-like particles as a result of the

accumulation of nanoleaves generated by nanoparticles from the effect of heat treatment at 623K. We noticed that when the number of shots 2000, the nanoparticles take the form of nanorods with a diameter ranging from 50 to 150 nanometers with an increase in the number of shots to 3000 afte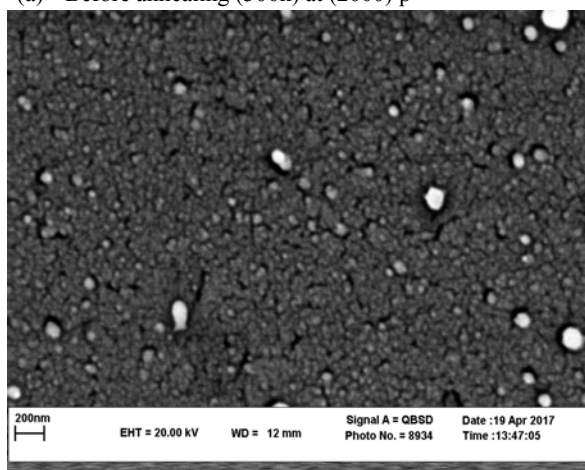r annealing at 623K as illustrated by Figure(7) (b) and (c) respectively, which are confirmed by XRD results. Annealing of particles at various temperatures could result in the agglomeration of particles as shown in Figure(4). At higher annealing temperatures, the nanoparticles are merging with each other forming a neck between the two particles.
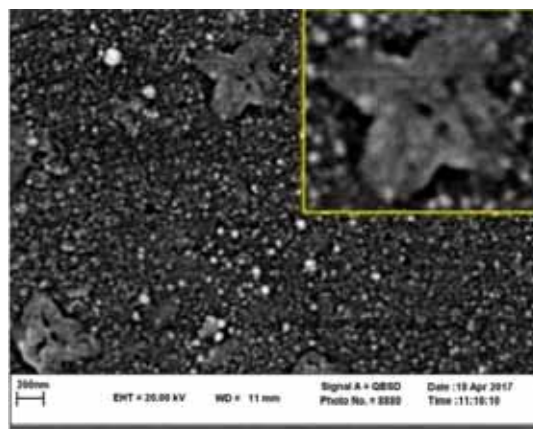

(a) Before annealing (300k) at (1000) p

After annealing (623k) at (1000) p nanoflower
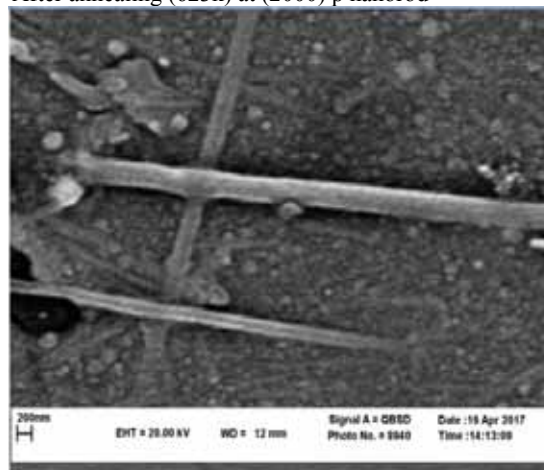

(a)   Before annealing (300k) at (2000) p

After annealing (623k) at (2000) p nanorod

(c) Before annealing (300k) at (3000) p

After annealing (623k) at (3000) p nanorod

Figure (7): SEM images of ZnS NPs thin films, the particles are shown for 1000 shots (a); and for 2000 shots (b); and for 3000 shots (c) at (300K) and annealing (623K)

Table (1): surface roughness of ZnS NPs films prepared at temperature (300k) and (623k)

Preparation temperature (K)	No. of laser shots	Root mean square surface roughness (nm)	Dislocations density(δ) (nm)$^{-2}$
As grown at (300K)	1000	3.61	0.0142
	2000	7.78	0.0103
	3000	8.36	0.0089
After annealing at (623K)	1000	0.674	0.0091
	2000	3.17	0.0059
	3000	7.47	0.0029

Interference peaks in the Figure (8). explained the uniform of the ZnS NPs films at 300K and the transmittance was found to increase with increasing number of shots of laser. After annealing at 623K.
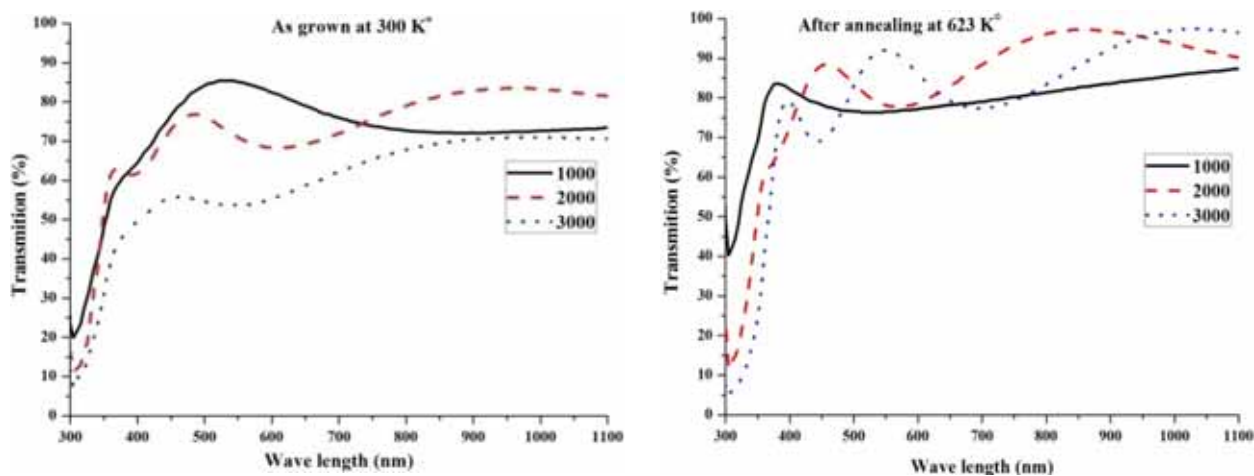
The direct energy band gap (E$_g$) was estimated from transmittance data as a function of wavelength using the relation [17]; $\alpha h\nu = \left(h\nu - E_g\right)^{\frac{1}{2}}$, where $h\nu$ is the photon energy (eV). The energy gap (E$_g$) of ZnS NPs films prepared at 300K and 623K calculated by extrapolating the linear part of $(\alpha h\nu)^2$ vs. $(h\nu)$ curves to $(\alpha h\nu)^2$=0 as shown in the Figure (9).

The band gap values estimated in this work for annealed ZnS NPs films at 623K (3.569, 3.488, 3.377 eV) are found to be higher than that prepared at 300K (3.557, 3.449, 3.319 eV), which may be linked with the structural changes causing quantum confinement effects in the ZnS NPs films as shown in Figure(10).

Also, the decrease in the values of E$_g$ by increasing number of laser shots (1000, 2000, 3000) is due to the increase in the crystal size of ZnS NPs. Photoluminescence (PL) spectrum of ZnS NPs films, which was prepared with a number of laser shots (1000) and flounce (16.98 J/cm^2) at (300K) and annealed at 623K, was measured in the region from 350 to 700 nm with excitation wave length (350 nm). Figure(11) shows ZnS NPs films grown (300K) and there are two evident peaks that give the ultraviolet (UL) and blue luminescence (BL) emission bands at 396 and 437 nm, respectively.

After annealing at 623K, these bands were quenched and shifted to 397 and 439 nm respectively as shown in Table (2).

This emission bands originated from zinc oxide and sulfur vacancies. The quenching of (PL) was attributed to the oxidation of sulfur into sulfate and the removal of lattice defects by the annealing process.

Figure (8): Optical transmission of the ZnS NPs films prepared at 300K and annealed temperature (623K)
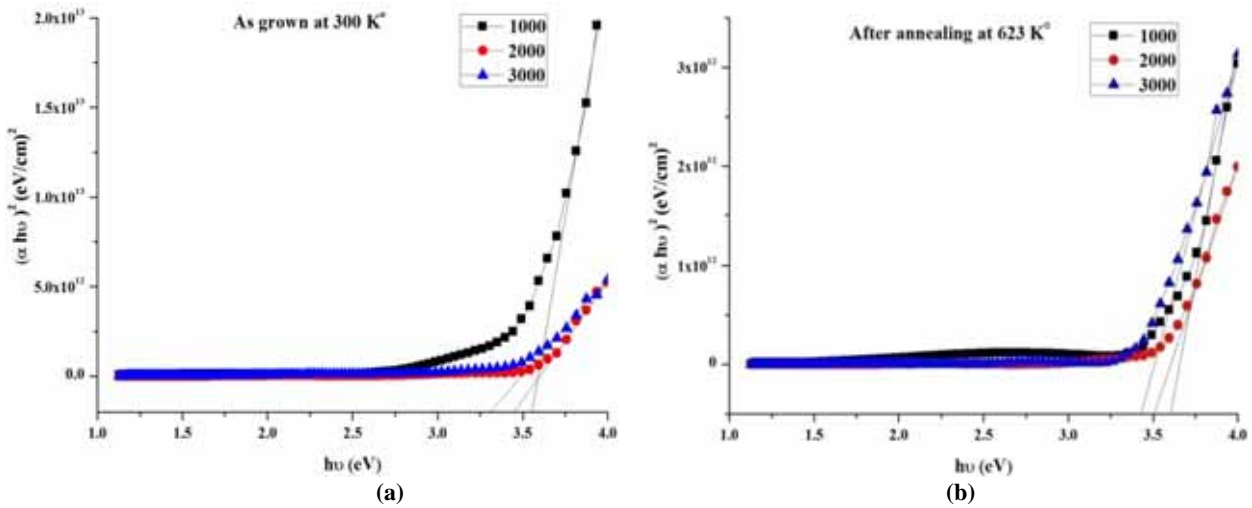
Figure (9): The energy gap (E_g) of ZnS NPs films prepared at (a) 300K and (b) 623K
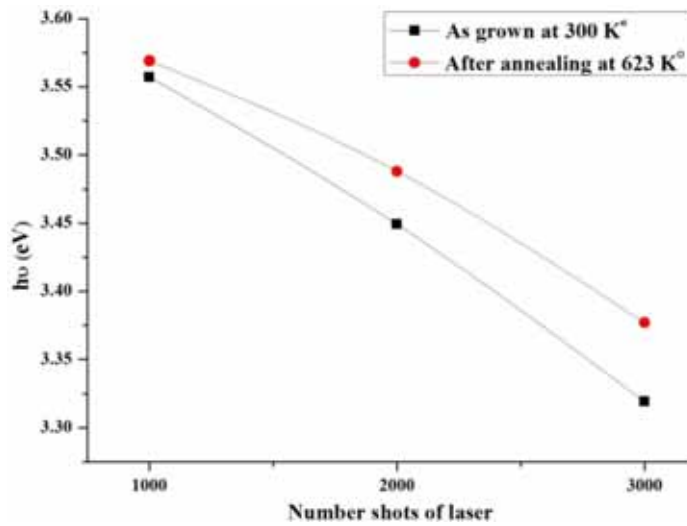

Figure (10): The E_g of ZnS NPs films prepared at temperature 300K and 623K
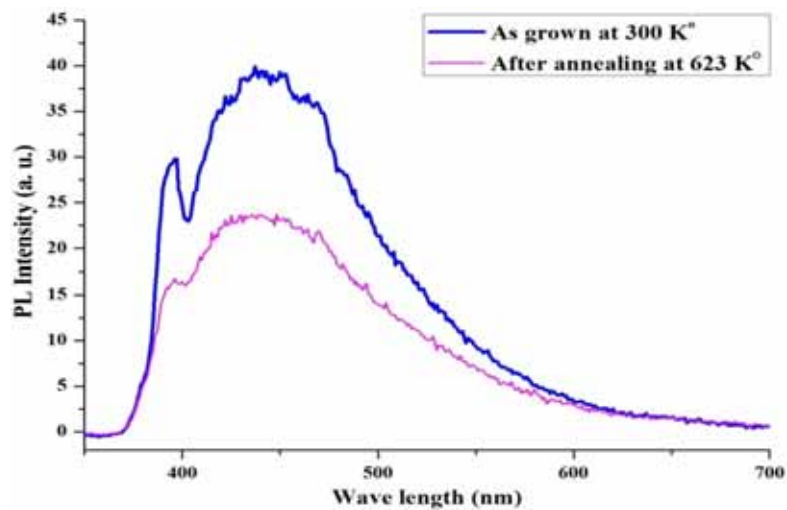

Figure (11): Room temperature Photoluminescence spectra of ZnS NPs films prepared and annealed at (300K) and (623K) respectively

Table (2): (UL) and (BL) of ZnS NPs films prepared at temperature (300k) and (623k)

Preparing temp. (K)	PL	FWHM (nm)	Intensity	λ (nm)
As grown (300K)	UL	62	29.8	396
	BL	111	38.6	437
Annealing temp. (623K)	UL	77.5	16.6	397
	BL	118	23.2	439

Conclusion

1 - From the absorbance spectra for ZnS thin films, it is concluded that the maximum absorption peaks shift towards the smaller wavelength with the increase of annealing temperatures. The value of absorption and reflection decreases with the increases of annealing temperatures whereas the transmission increases.

2- The optical energy gap for ZnS increases with the increase in the annealing temperatures.

3- Increasing number pulses of laser on the samples leads to increased roughness of the surface and increased temperature reduces.

4- ZnS NPs films at 300 K° and the transmittance increased after annealing at 623 K with increasing number pulses of laser.

5– The grain size increases with the increase of absorption.

6- The surface was uniformly covered and the observed surface properties have a strong effect on the optical properties of thin films such as transition, absorption, and reflection.

7– The absorption coefficient (α) > 10^4 cm^{-1} indicates direct transitions.

8– Film annealing leads to improving crystallinity, increasing of the grain size and eliminating some defects from the films.

9- The carrier concentration decreases with the increase of annealing temperatures, and the carrier mobility increases with the increase of annealing temperatures.

References

1- A. Nitta , K. Tanakab, Y. Maekawab, M. Kusabirakib, and Masao Aozasa, Effects of gas impurities in the sputtering environment on the stoichiometry and crystallinity of ZnS: Mn electroluminescent-device active layers, Thin Solid Films. 384(2001), 261-268.

2- S. Yano, R. Schroeder, B. Ullrich, and H. Sakai, Absorption and photocurrent properties of thin ZnS films formed by pulsed-laser deposition on quartz, Thin Solid Films. 423(2003) 273–276.

3- Q.J. Feng, D.Z. Shen, J.Y. Zhang, H.W. Liang, D.X. Zhao, Y.M. Lua, and X.W. Fan, Highly aligned ZnS nanorods grown by plasma-assisted metalorganic chemical vapor deposition, J. Crystal Growth. 285(2005) 561–565.

4- S. Wang, X. Fu, G. Xia, J. Wang, J. Shao, and Z. Fan, Structure and optical properties of ZnS thin films grown by glancing angle deposition, Appl. Surf. Sci., 252 (2006) 8734–8737.

5- N. Fathy, R. Kobayashi, and M. Ichimura, Preparation of ZnS thin films by the pulsed electrochemical deposition, Mater. Sci. Eng. B. 107(2004) 271–27.

6- P. Roy, J.R. Ota, and S.K. Srivastava, Crystalline ZnS thin films by chemical bath deposition method and its characterization, Thin Solid Films. 515(2006) 1912-1917.

7- W.L. Davidson, Xray diffraction evidence for ZnS formation in zinc activated rubber vulcanizates. phys Rev. 74(1948) 116-117.

8- S.Biswas, S.kar, abrication of ZnS nanoparticles and nanorods with cubic and hexagonal crystal structures : a sample solvothermal approach, Nanotechnology. 19 (2008) 045710.

9- H. wany D. Ahnj Huik, H. Sony, Structural and optical Properties of ZnS thin films deposited by RF magnetron suputtering, Nanoscale Reslett. (2012) 7-26.

10- D. Hariskos, B. Fuchs, R. Menner, N. Naghavi, Hubertc, D. Lincot, M. powalia, The Zn(S,O,OH)/ZnMgo buffer in thin film Cu(In, Ga)(Se,S) 2-based solar cell part ll : magnetron suppttering of the ZnMgo buffer layer for in – line Co- evaporated Cu(In, Ga) Se2 solar cells prog photovolt pes" 17 (2009) 479-488.

11- X.S. Fxany, H. Yec, X.S. Peng, Y.H. wang, W. Uyc, L.D. Zhang, Large- scale synthesis of ZnS nanosheets by the evaporation of ZnS nanopowders, J cryst Growth. 263 (2004) 263-268.

12- X. YWang, C. Zhuy, H. Fan, M.F Zhang, X. Ibj, H. Zwang, Growth of ZnS Microfans and nanosheets : Controllable morphology and phase, J. cryst Growth. 310 (2008) 2525-2531.

13- A. Ichiboshi, M. Hongo, T. Akamine, T. Dobashi, T. Nakada, Ultrasonic chemical bath depost of ZnS(O,OH) buffer layers and its application to

CIGS thin film solar cells, sol energy mater So: cells. 90 (2006) 3130-3135.

14- A. Inamet, Low magnetic flux noise observed in laser deposited in situ films of   yB2 Cu3Oy and implications for high – TC SQUIDS". In: Nature 341 O, pp. (1980) 723 – 726

15- W.H. Bloss, F. Plisterer, H.W. Schock, Advances in Solar energy, and Annual review of research & development. Vol. 4(1988) P-275.

16- C. Suryanarayana, M. GNorton, X-ray diffraction a practical approach, New York: Plenum Press; 1998.

17- M. Ethayaraja, C. Ravikumar, D. Muthukumaran, K. Dutta, R.J. Bandyopadhyaya, CdS-ZnS core-shell nanoparticle formation: Experiment mechanism and simulation, J. Phys. Chem. 111 (2007) 3246-3252.